Stable Biopassive Insulation Synthesized by Initiated Chemical Vapor Deposition of Poly(1,3,5-trivinyltrimethylcyclotrisiloxane)

W. S. O'Shaughnessy,[†] S. K. Murthy,[‡] D. J. Edell,[§] and K. K. Gleason*,[†]

Department of Chemical Engineering, Massachusetts Institute of Technology, Cambridge, Massachusetts 02139, Department of Chemical Engineering, Northeastern University, Boston, Massachusetts 02115, and Innersea Technology, Inc., Bedford, Massachusetts 01730

Received February 28, 2007; Revised Manuscript Received April 24, 2007

The permanent implantation of electronic probes capable of recording neural activity patterns requires long-term electrical insulation of these devices by biopassive coatings. In this work, the material properties and neural cell compatibility of a novel polymeric material, poly(trivinyltrimethylcyclotrisiloxane) (poly(V_3D_3)), are demonstrated to be suitable for application as permanently bioimplanted electrically insulating films. The poly(V_3D_3) polymeric films are synthesized by initiated chemical vapor deposition (iCVD), allowing for conformal and flexible encapsulation of fine wires. The poly(V_3D_3) also exhibits high adhesive strength to silicon substrates, a common material of manufacture for neural probes. The poly(V_3D_3) films were found to be insoluble in both polar and nonpolar solvents, consistent with their highly cross-linked structure. The films are pinhole-free and extremely smooth, having a root-mean-square (rms) roughness of 0.4 nm. The material possesses a bulk resistivity of 4×10^{15} Ohm-cm exceeding that of Parylene-C, the material currently used to insulate neurally implanted devices. The iCVD poly(V_3D_3) films are hydrolytically stable and are demonstrated to maintain their electrical properties under physiological soak conditions, and constant electrical bias, for more than 2 years. In addition, biocompatibility studies with PC12 neurons demonstrate that this material is noncytotoxic and does not influence cell proliferation.

1. Introduction

The field of neuroprosthetics utilizes the firing patterns of individual neurons to control electronic devices external to the subject. Recent advances in this field, including a human implant trial,[1,2] have brought the possibility of therapeutic implementation into the near term. However, one major barrier to clinical use remains the long-term stability of the neural arrays within the brain.[3−11] Of paramount importance to this stability is the electrically insulating coating placed on the device prior to implantation. Each neural array consists of 10−100 neural probe shanks, each 25−50 μm in diameter but millimeters in length.[12−16] These high aspect ratio features make the application of a smooth, even coating a significant challenge. In addition, the coating must be highly electrically resistive to insulate the implant with as little increase in the diameter of the probe shanks as possible. The coating must be conformal and adherent to the device for corrosion prevention over the 20+ year implant design life. The coating properties must also be retained within the implantation environment while not inducing a negative biological response.[17] The material should possess some mechanical flexibility so that both the probe array and its lead wires can be concurrently insulated to maximize device reliability. For concurrent insulation, the coating material must adhere to both probe substrate materials, such as silicon, and metallization materials, such as gold and copper.

While there are many different methodologies available for the application of insulating biomaterial coatings, the above requirements make chemical vapor deposition (CVD) an ideal approach.[18−24] CVD is a coating process which is known to produce conformal, pinhole-free films of controllable thickness on 3-D substrates.[19,25,26] As CVD is an all dry process, coating problems associated with nonuniform wetting because of surface tension effects, which can be exacerbated on high aspect ratio substrates, are avoided.[27] In addition, there is no issue of entrained solvent in the coating, a significant cause of polymer implant rejection.[17] To exploit the advantages of vapor deposition while not sacrificing control over polymer chemistry, initiated CVD (iCVD) can be utilized. The iCVD method employs a free-radical generating initiator to begin vapor-phase polymerization of a vinyl monomer under much more benign conditions than pulsed plasma, thermal, or traditional hot filament CVD.[28−32] This allows for both a high degree of control over polymer chemistry, as with solution-phase polymer synthesis, and the retention of sensitive functional groups within the resulting films not possible through traditional CVD methods.[30,33] In addition, copolymer films and films of graded composition can be created through iCVD, allowing for independent optimization of the bulk and surface properties of deposited coatings.

In this work, the material properties, biocompatibility, and long-term stability of poly(1,3,5-trivinyltrimethylcyclotrisiolxane), poly(V_3D_3), are evaluated. This material has been developed as an iCVD synthesized polymer for the insulation of neural recording arrays. While the polymerization mechanism and molecular structure of poly(V_3D_3) have been previously described in detail,[33] the creation of thin films of this polymer is not possible by techniques other than iCVD because of both solubility and steric considerations. Its structure is composed of carbon backbone chains joined together by siloxane rings. The density of cross-linking within this material combined with the retention of siloxane ring moieties present in the monomer prevents the formation of this molecular structure through either

* Author to whom correspondence should be addressed. E-mail: kkg@mit.edu

[†] Massachusetts Institute of Technology.

[‡] Northeastern University.

[§] Innersea Technology Inc.

10.1021/bm070242s CCC: $37.00
Published on Web 06/26/2007

Table 1. Reactor Conditions for Deposition of iCVD Polymer Films

label	pressure (mTorr)	stage temperature (K)	filament temperature (K)	monomer flow rate (sccm)	initiator flow rate (sccm)
A	350	328	773	5	0.5
B	350	333	773	5	0.5
C	350	353	773	5	0.5
D	450	333	773	5	0.5
E	350	308	773	5	0.5

solution-phase polymerization or noninitiated CVD. Also, the polymer structure has structural features of both polyethylene (PE), in the long backbone chains, and of polysiloxane in the cross-linking rings. As such, it is likely to behave as a copolymer of these two well-characterized biomaterials, inspiring its use for this application. Siloxane bonds are noted for their flexibility. Hence, incorporation of siloxane rings may avoid brittle failure even in films which are highly cross-linked. Additionally, the siloxane rings are likely to inhibit the formation of PE crystallites.

2. Experimental Section

2.1. Sample Preparation. Polymer depositions were performed in a custom-built vacuum chamber (Sharon Vacuum) as previously described.[29,31] Briefly, the deposition chamber is a 240 mm diameter cylinder with a height of 33 mm. The top of the reactor is covered with a 25 mm thick quartz plate, allowing for observation of the sample throughout deposition. Liquid monomer (1,3,5 trivinyl-trimethyl-cyclotrisiloxane, 99% Gelest) and initiator (tertbutyl peroxide, 98% Aldrich) were utilized without further purification. The monomer was vaporized in a metal crucible maintained at 80 ± 2 °C, and vapor flow was metered to the reactor through a mass flow controller (Model 1152, MKS). The initiator was placed in a sealed Pyrex container at room temperature, and vapors were fed to the reactor through a second mass flow controller (Model 1179A, MKS). Gaseous monomer and initiator were premixed and fed through a port in the side of the reactor cylinder where they then passed through a distribution baffle plate to ensure uniform flow over the deposition area.

Within the reactor, a resistively heated filament array, 20 mm above the substrate, was utilized to breakdown the initiator into radical species. Filament temperature was measured by a thermocouple (Type K, AWG 36, Omega Engineering) directly attached to one of the filament wires. Pressure within the chamber was measured by a capacitance diaphragm gauge and was controlled through use of a throttling butterfly valve (Intellisys, NorCal) connected to an autotuned digital controller (Intellisys, NorCal).

Samples were deposited on either 100 mm diameter IR transparent silicon wafers (WaferWorld) or 50 μm diameter gold wire in direct contact with a backside cooled substrate stage within the reactor. To remove contaminants, all silicon samples were ultrasonicated for 10 min in deionized water, were rinsed with isopropyl alcohol, and were dried with nitrogen. Substrate temperature was maintained with an accuracy of ±2 °C throughout the deposition by circulation of heated silicon oil. Film growth was observed in situ through use of a 633 nm laser source (JDS Uniphase), with reflectance intensity measured by a Metrologic detector. Interferometric cycle thickness was calibrated using ellipsometer modeling as described below.

Table 1, below, shows reactor conditions for all iCVD film samples analyzed in this paper.

2.2. Material Testing. Dielectric measurements were made using a mercury probe (Materials Development Corp.) driven by a Keithley 236 source measurement unit. A capacitance versus voltage curve was generated, and the dielectric constant was calculated from the accumulation capacitance of the sample. Sample thickness and refractive index were measured through the use of a variable angle spectroscopic ellipsometer (J.A. Woollam M-2000, xenon light source). A Cauchy-Urbach model was utilized to obtain a nonlinear least-squares fit of data obtained at 3 (65°, 70°, 75°) angles and 225 wavelengths. Electrical resistance measurements were made utilizing a Keithley 617 Electrometer attached to the sample by adhesive electrodes (Tyco Healthcare) of known contact area. Sample resistivity was then calculated by multiplying the measured resistance by the ratio of the electrode area to the sample thickness (as determined by spectroscopic ellipsometry). Solubility testing was performed by immersion of thin film samples, on silicon substrates, in the stated solvent for 30 min, followed by drying with room-temperature nitrogen. Film thickness was measured by spectroscopic ellipsometry before and after immersion.

Coating adhesion to silicon wafer substrates was determined using ASTM tape test D3359-02. For this adhesion test, a grid of 1 mm squares was cut into the sample and adhesive tape (P99 polyester tape, Pemacel) was applied and rapidly removed. The sample was then visually inspected to determine if any loss of adhesion between any of the small squares of coating and the surface had occurred. Testing was performed before and after boiling coated silicon wafer samples in deionized water for 60 min.

Fourier transform infrared spectroscopy (FTIR) was performed on a Nicolet Nexus 870 ESP spectrometer in normal transmission mode. A DTGS KBr detector was utilized over the range of 400−4000 cm^{-1} with a 4 cm^{-1} resolution. Measurements were averaged over either 64 or 128 scans. All samples were baseline corrected, and thickness was normalized to allow for accurate comparison. Scanning electron micrographs were generated using a FEI/Phillips XL30 FEG ESEM in environmental scanning mode. ESEM samples were examined as deposited, without addition of an evaporated metal overcoat. Atomic force microscopy (AFM) was performed on a Digital Instruments 3100 AFM with a type 4 controller utilizing a sample area of 1.5 μm by 1.5 μm.

Electrically biased soak testing was performed by Innersea Technology Inc. (Bedford, MA). Briefly, samples were deposited on a single side of 1 cm^2 pieces of silicon wafer to a thickness of 5 μm. To remove contaminants, samples were ultrasonicated for 10 min in deionized water, were rinsed with isopropyl alcohol, and were dried with nitrogen prior to coating deposition. Each square was then attached to a backside electrode, and the sides and the back of the sample were insulated using silicone rubber to ensure that current could only pass to the backside electrode through the deposited coating. Samples were then placed on leads and were suspended in test tubes filled with saline solution as shown in Figure 1. Each tube was also fitted with an electrode suspended in the saline solution, and a sweeping electrical bias of +5 V to −5 V was maintained between this free electrode and those present on each of the samples under test. The leakage current through each of the samples was then measured every 24−72 h at both +5 V and −5 V, and sample electrical resistance was subsequently calculated and recorded.

2.3. Neuron Compatibility Testing. Coated glass slides were placed in suspensions of PC12 cells over a period of 12 days. The PC12 cell line was obtained from American Type Culture Collection (ATCC) and was cultured in F-12K medium (ATCC) supplemented with 15% horse serum (ATCC), 2.5% fetal bovine serum (BioWhittaker), and 25 units/mL penicillin-streptomycin (Hyclone) at 37 °C and 5% CO_2. For neurocompatibility experiments, five coated glass slides were placed in small polystyrene Petri dishes (Fisher; one slide in each dish) along with 12 mL of cell suspension in each dish. Five uncoated glass slides in similar Petri dishes served as controls. Cell culture conditions utilized for this study provided for the growth of PC12 neurons in suspension above the substrates, though contact due to cell settling did occur. The cell concentration in each dish was monitored over a 12 day period, with measurements taken every other day. Medium changes were carried out in each Petri dish every 3 days. For each time point, the

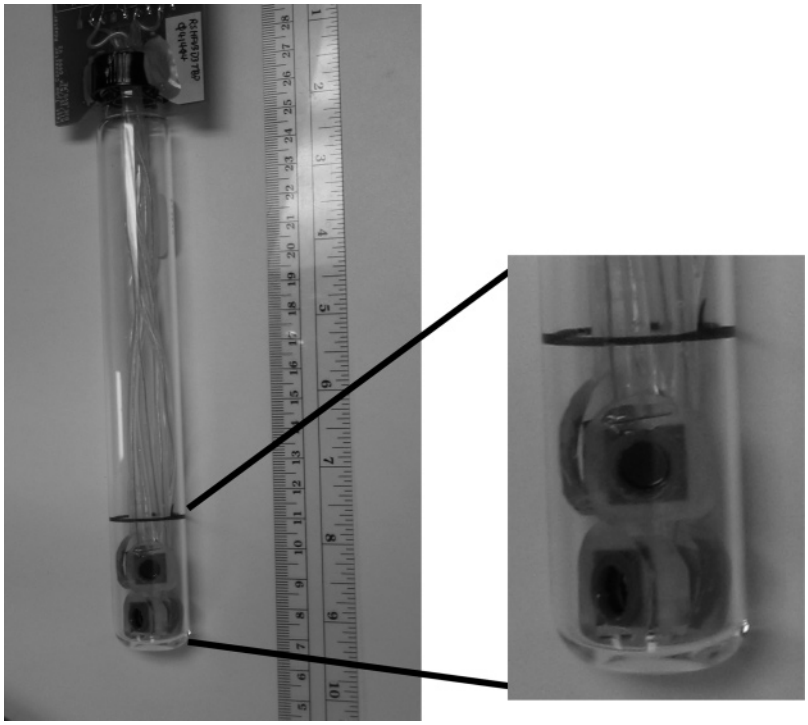

Figure 1. Electrically biased saline soak test setup for durability testing of poly(V_3D_3) coatings. Enlargement shows detail of how samples were assembled and electrically isolated.

Table 2. Optical and Electrical Properties of Poly(V_3D_3) along with Those of Polyethylene, Polydimethylsiloxane, and Parylene-C for Comparison[37,38]

material	dielectric constant	refractive index	resistivity (Ω-cm)
poly(V_3D_3)	2.5 ± 0.2	1.465 ± 0.01	$4 (\pm 2) \times 10^{15}$
polyethylene	2.3 ± 0.02	1.49−1.54	1×10^{14}
polydimethylsiloxane	2.6 ± 0.2	1.40	1×10^{16}
parylene-C	3.0 ± 0.15	1.64	1×10^{15}

Table 3. ASTM Tape Test D3359-02 Adhesion Data for Poly(V_3D_3) Deposited on Silicon Wafer Substrates[a]

sample thickness	rating (as deposited)	rating (after boiling)
61 ± 2 nm	5B	5B
	(0% removal)	(0% removal)
315 ± 6 nm	5B	5B
	(0% removal)	(0% removal)

[a] 5B rating indicates best possible adhesion to substrate as measurable by this assay. Measurements were taken before and after boiling in deionized water for 60 min.

cell concentration from the five samples (or controls) was averaged for the plot in Figure 6, and the error bars represent the standard deviation of the data.

3. Results and Discussion

3.1. Physical Properties. Table 2 shows optical and electronic property data for poly(V_3D_3) film "B" (Table 1) along with values for PE and PDMS included for reference. As expected, all properties of the new material fall between those of PE and PDMS, confirming the assertion that the material will behave as a PE−siloxane copolymer. Of these properties, the most important to the application is the electrical resistivity. To both ensure recording from single neurons and increase recording sensitivity, the electrical resistance of the passivation coating should be as high as possible. Parylene-C, the current electrical insulation material of choice for these implants,[16,34−36] has a bulk resistivity of about 10^{15} Ω-cm, slightly lower than that of the poly(V_3D_3). This differential should allow for deposition of thinner passivation coatings that will provide the same level of electrical insulation to the device.

The material properties of poly(V_3D_3) were found to be insensitive to changes in deposition conditions over the range of conditions reported in Table 1, samples A−D. The only exception appears to be when substrate temperatures are reduced below a reactor pressure dependent threshold value. For a deposition pressure of 350 mtorr, this threshold was observed to be ~323 K. Below this level, a decrease in bulk resistivity of up to 2 orders of magnitude is observed. A resistivity of $\sim 1 \times 10^{13}$ Ohm-cm was obtained for samples deposited at a stage temperature of 308 K (condition E, Table 1). The loss of electrical resistance is hypothesized to originate with the entrainment of some small molecules in the polymerized film when surface temperature is low. Upon reactor blowdown following the deposition process, vaporization of the entrained molecules leads to defects which can be observed by optical microscopy as micrometer-size disk-shaped voids in the coating. The entrained small molecules could be either short oligomers of the polymer or possibly a single monomer unit which has been initiated and terminated without further monomer addition. Condensation of the pure monomer is less likely, as the partial pressure of monomer in the reactor, 280 mTorr, is significantly below its vapor pressure of ~500 mTorr at the substrate temperature.

Table 3 presents data on the adhesion of poly(V_3D_3) films, "B" (Table 1), to silicon wafer substrates. The native oxide was not removed prior to the iCVD coating step. Substrate adhesion is very important for the long-term stability of implanted probes as coating delamination can quickly lead to corrosion and device failure.[39] Coating adhesion was evaluated for films both less than and greater than 100 nm in thickness, since the organizational structure of polymer films deposited on crystalline

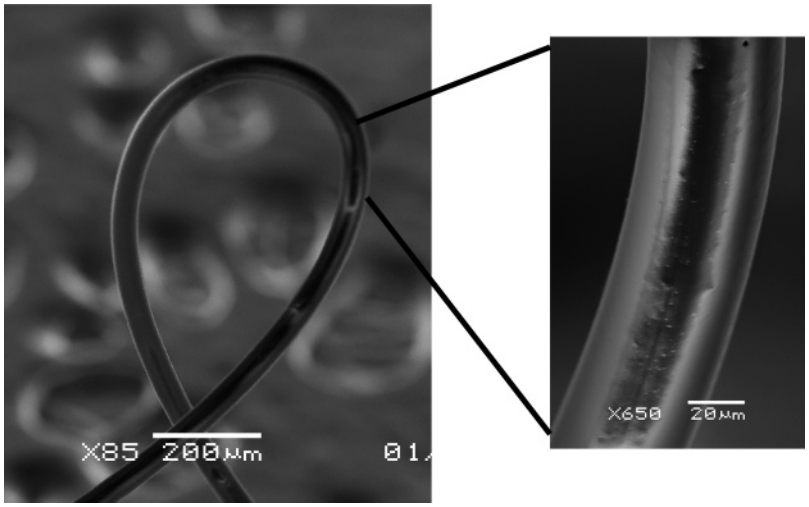

Figure 2. Scanning electron micrograph of 50 μm diameter gold wire coated with 2−3 μm of poly(V_3D_3). Wire is bent into a ~250 μm diameter loop without evidence of film cracking or buckling. Enlargement shows e-beam ablation of the coating as well as a lack of cracking or buckling at higher magnification.

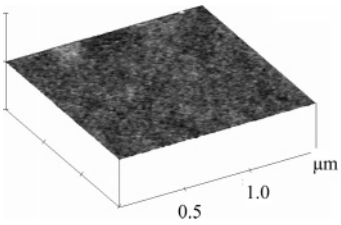

Figure 3. Atomic force micrograph of poly(V_3D_3) film "C" deposited on a silicon wafer. Sample has an overall rms roughness of 0.4 nm with a peak-to-peak roughness of <0.9 nm.

substrates has been reported to be greatly affected by the crystalline lattice structure in the first 50−200 nm.[40,41] In all cases, a rating of 5B, no loss of coating adhesion observable, was obtained from ASTM tape test D3359-02. To make an initial assessment of whether long-term immersion in an aqueous environment would impact adhesion, samples were then boiled for 30 min in deionized water. Once again, no loss of film adhesion was observed upon testing.

Figure 2 displays a scanning electron microscopy (SEM) image of a nominally 50 μm diameter gold wire coated with 2−3 μm of poly(V_3D_3) deposited at condition B from Table 1. The wire has been bent into a loop of ~250 μm in diameter to demonstrate the flexibility of the thin film coating. As can be seen from the figure, no cracking or buckling in the film is observable in either the SEM or the inset enlargement. In addition, the enlargement demonstrates how the material can be ablated through e-beam patterning, a necessary property to allow for the exposure of recording sites on a neural probe subsequent to coating. Flexibility is an important property for the coating of neural probe assemblies which typically have multiple lead wires attaching them to either locally implanted or external electronics. The ability to coat these leads along with the device would be a significant advantage over Parylene-C which is too brittle for such an application.[36] The flexibility of the poly(V_3D_3) is not surprising when the polymer film is considered as a siloxane copolymer. Siloxane materials are noted for their flexibility and elastomeric properties.

Figure 3 presents an atomic force micrograph (AFM) of poly(V_3D_3) film "C" (Table 1) deposited on a silicon wafer substrate to thickness of ~250 nm. The overall root-mean-square (rms) roughness of the sample is only 0.4 nm, comparing well to the 0.15 nm observed for polished silicon wafers. In addition, the peak-to-peak roughness (not shown) is no greater than 0.9 nm.

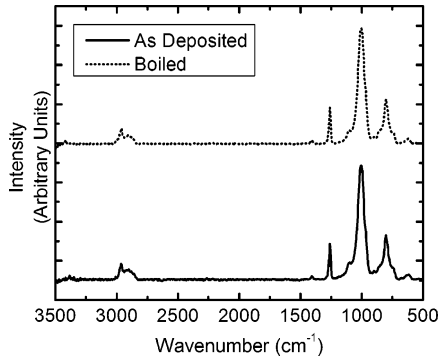

Figure 4. FTIR spectra of a poly(V_3D_3) film B before and after boiling for 60 min in deionized water. No change in spectra is apparent.

This indicates that the low rms figure is due to a film of uniformly low surface roughness, not a smooth film with occasional large peaks/flaws. This is important to ensure that no point imperfections are present in the film. Additionally, while the AFM data was obtained from analysis of a sample deposited at condition C, there was very little variation in surface roughness observed in samples deposited at conditions listed in Table 1. All tested samples were within ±0.25 nm rms roughness of the above data. The low roughness of thin films of the polymer is indicative of an amorphous material, though confirmation of this through X-ray powder diffraction (XRD) or differential scanning calorimetry (DSC) is not possible because of the small sample sizes. An amorphous film is also consistent with the interpretation of the chemical structure as a PE−siloxane copolymer. While PE is a semicrystalline polymer, it is theorized that the presence of the siloxane side groups within the poly(V_3D_3) would most likely prevent the PE chains from forming crystalline domains. These observations are also consistent with the film flexibility observed in Figure 2; a semicrystalline material would be likely to display some degree of brittle cracking under strain. An amorphous polymer structure is beneficial for electrically insulating films as material properties will be isotropic, and the possibility of locally high electrical conduction at crystalline grain boundaries is avoided.

3.2. Material Stability. Figure 4 displays two FTIR spectra of a poly(V_3D_3) film deposited at condition B. The bottom spectra is that of the as-deposited film, while the top spectra is of the same film after boiling at atmospheric pressure in deionized water for 1 h. A detailed analysis of the IR absorptions

Table 4. Film Thickness of Samples before and after 30 min Soak in Specified Solvent[a]

solvent	initial thickness	final thickness
deionized water	391 ± 8 nm	397 ± 8 nm
isopropyl alcohol	410 ± 12 nm	408 ± 12 nm
acetone	418 ± 10 nm	424 ± 10 nm
dimethyl sulfoxide	438 ± 8 nm	431 ± 8 nm
tetrahydrofuran	292 ± 6 nm	293 ± 6 nm

[a] Thickness measured by spectroscopic ellipsometry with accuracy given.

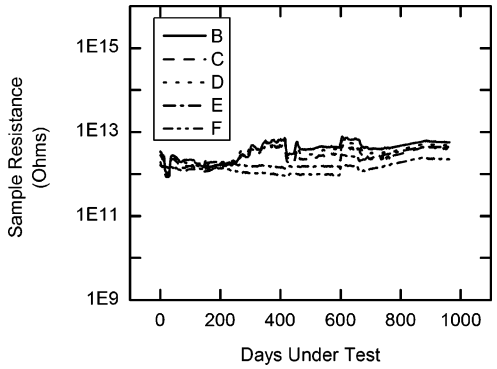

Figure 5. Electrical resistance of poly(V_3D_3) samples under simulated bioimplanted conditions and constant electrical bias. Samples show no degradation in electrical resistance over a period of greater than two-and-a-half years.

present has been previously reported.[33] No change in FTIR spectra of the material is observed, indicating that there are no hydrolytically labile moieties present in the film which could be degraded over time in an aqueous environment. Were the film to react with water, new absorptions associated with hydroxyl groups would be observed between both 3400−3600 cm^{-1} and 1000−1100 cm^{-1}.[42] The hydrolytic stability of this material is not unexpected when again considering the poly(V_3D_3) within the context of a PE−siloxane copolymer. Both components are unaffected chemically by aqueous environments.

Table 4 presents solubility data on poly(V_3D_3) films prepared at condition "A" in a variety of common solvents. Resistance to polar solvents is obviously of most importance for permanently implantable materials. However, cholesterols and other fatty acids in the blood can act as nonpolar solvents, slowly leaching away oil-soluble materials. As shown by the data, poly(V_3D_3) films show no solubility in either polar or nonpolar solvents, indicating that coating loss because of solvation within the body will not likely be a factor. These results confirm that the cross-linked structure of the poly(V_3D_3) films is effective in retaining all deposited material and that low molecular weight chains, which would be solubilized, are not present.

Stability of coating electrical properties under physiological conditions is of paramount importance for the application. Figure 5 presents a plot of electrical resistance versus time for five thin film poly(V_3D_3) samples from June 2004 through February 2006. These samples were deposited at condition B (Table 1). As described in section 2.2, these samples were immersed in physiological saline and had a constant sweeping electrical bias of +5 V to −5 V applied across them. Because of film area versus film thickness considerations, a resistivity of 10^{15} Ω-cm corresponds to a measured resistance of 1.1×10^{12} Ω, indicating that all five samples fall in the range of electrical resistivity previously presented in Table 2. These data indicate that, even after more than two-and-a-half years of simulated implantation,

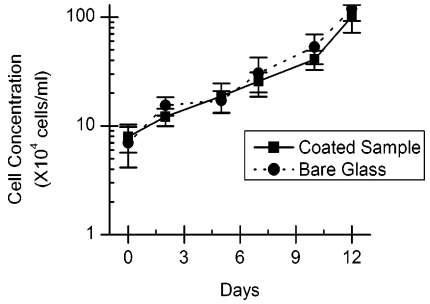

Figure 6. PC12 neuron growth in the presence of uncoated and poly(V_3D_3) coated glass substrates. No significant difference in cell growth is observed, indicating that poly(V_3D_3) is noncytotoxic to PC12 neurons.

the electrical properties of the five samples have not degraded. Indeed, the small variations in resistance observed seem to track between the samples, indicating that the changes are more likely because of small fluctuations in calibration of the electrometer utilized to take the measurements. Three additional samples were placed under test along with these five, and all three failed electrically within the first two weeks. Examination of these failed samples indicated that they were point failures because of the presence of particulate contaminants on the substrate surface prior to coating and were not failures because of degradation of the coating itself. This particulate contamination likely occurred after sample cleaning procedures as depositions were not performed in a clean room environment. Such an environment will be utilized during future neural implant device manufacture to avoid this failure mode.

3.3. Neuron Compatibility. The compatibility of poly(V_3D_3) thin films to neurons was assessed by culturing PC12 neurons in the presence of glass slides coated with the material. PC12 cultures in the presence of uncoated glass slides served as a negative control. Figure 6 shows the progression of cell concentration as a function of time over a 12 day period. There is no statistically significant (as evaluated by 95% confidence *t*-test[43]) difference between sample and control cell concentration data, indicating that contact with poly(V_3D_3) does not affect the growth characteristics of PC12 neurons. In both sample and control, the PC12 cells retained a rounded morphology and did not adhere to the dish or glass surfaces. This behavior is consistent with the expected behavior of PC12 cells in the presence of serum but in the absence of cell adhesion proteins or neurotrophic factors.[44] While this growth curve experiment is a first-order assay for biocompatibility, the results nevertheless indicate that poly(V_3D_3) films do not retard cell growth because of factors such as cytotoxic chemical groups, entrained monomers, or unreacted initiator. Additionally, previous work with related film chemistries has demonstrated the tethering of bioactive molecules, such as the peptide sequence RGD, to the surface of iCVD films through vinyl moieties not consumed during polymerization.[45] This or related approaches can be utilized to further increase the biocompatibility of poly(V_3D_3).

4. Conclusions

In this work, thin films of poly(V_3D_3) deposited by iCVD have been demonstrated to possess the material properties and long-term stability required for use in electrically insulating neural recording arrays. The material has also been shown to have excellent adhesion to silicone substrates and a high degree of flexibility, both necessary properties for an ideal neural probe insulating material. It has been demonstrated that this polymer

in many ways behaves as a copolymer of polyethylene and a polysiloxane, as would be predicted from its chemical structure. Poly(V_3D_3) has a bulk electrical resistivity in excess of 10^{15} Ω-cm, allowing for films as thin as 5 μm to provide the required degree of electrical insulation for the application. This value falls between those observed in PE and PDMS, as do the refractive index and dielectric constant of the material. iCVD deposited poly(V_3D_3) shows no spectroscopic change because of hydrolysis when exposed to a 100 °C aqueous environment. Negligible solubility in a wide range of solvents has been demonstrated, assuring that the coating will not be dissolved by either hydrophilic or hydrophobic materials it may encounter when implanted in the cortex. In addition, it has been shown that the electrical properties of the material are maintained, with no degradation, for over two-and-a-half years under simulated implant conditions. Last, biocompatibility studies with PC12 neurons demonstrate that this material is noncytotoxic and does not influence cell proliferation. These data provide initial indications of biocompatibility.

Future work with this material will focus on both short- and long-term in vivo testing to better understand how the coating will behave in an active biological environment. In addition, the surface of the material will be modified for attachment of bioactive molecules, such as the peptide RGD, to increase cell affinity for the material surface. This modification will maximize the integration and stability of the coating within the cellular matrix after implantation.

Acknowledgment. The authors acknowledge the support of the NIH under contract No. NO1-NS2-2347. This work also made use of the MRSEC shared facilities supported by NSF grant No. DMR-9400334. The authors thank Anilkumar Achyuta for performing the cell compatibility experiments.

References and Notes

(1) Santhanam, G.; Ryu, S. I.; Yu, B. M.; Afshar, A.; Shenoy, K. V. A high-performance brain-computer interface. *Nature* **2006**, *442* (7099), 195−198.
(2) Taylor, D. M.; Tillery, S. I. H.; Schwartz, A. B. Direct cortical control of 3D neuroprosthetic devices. *Science* **2002**, *296* (5574), 1829−1832.
(3) Beard, R. B.; Hung, B. N.; Schmukler, R. Biocompatibility Considerations at Stimulating Electrode Interfaces. *Ann. Biomed. Eng.* **1992**, *20* (3), 395−410.
(4) Szarowski, D. H.; Andersen, M. D.; Retterer, S.; Spence, A. J.; Isaacson, M.; Craighead, H. G.; Turner, J. N.; Shain, W. Brain responses to micro-machined silicon devices. *Brain Res.* **2003**, *983* (1−2), 23−35.
(5) Edell, D. J.; Toi, V. V.; McNeil, V. M.; Clark, L. D. Factors Influencing the Biocompatibility of Insertable Silicon Microshafts in Cerebral-Cortex. *IEEE Trans. Biomed. Eng.* **1992**, *39* (6), 635−643.
(6) Vetter, R. J.; Williams, J. C.; Hetke, J. F.; Nunamaker, E. A.; Kipke, D. R. Chronic neural recording using silicon-substrate microelectrode arrays implanted in cerebral cortex. *IEEE Trans. Biomed. Eng.* **2004**, *51* (6), 896−904.
(7) Schmidt, S.; Horch, K.; Normann, R. Biocompatibility of Silicon-Based Electrode Arrays Implanted in Feline Cortical Tissue. *J. Biomed. Mater. Res.* **1993**, *27* (11), 1393−1399.
(8) Rousche, P. J.; Normann, R. A. Chronic recording capability of the Utah Intracortical Electrode Array in cat sensory cortex. *J. Neurosci. Methods* **1998**, *82* (1), 1−15.
(9) Polikov, V. S.; Tresco, P. A.; Reichert, W. M. Response of brain tissue to chronically implanted neural electrodes. *J. Neurosci. Methods* **2005**, *148* (1), 1−18.
(10) Rennaker, R. L.; Street, S.; Ruyle, A. M.; Sloan, A. M. A comparison of chronic multi-channel cortical implantation techniques: manual versus mechanical insertion. *J. Neurosci. Methods* **2005**, *142* (2), 169−176.
(11) Griffith, R. W.; Humphrey, D. R. Long-term gliosis around chronically implanted platinum electrodes in the Rhesus macaque motor cortex. *Neurosci. Lett.* **2006**, *406* (1−2), 81−86.
(12) Rutten, W. L. C. Selective electrical interfaces with the nervous system. *Annu. Rev. Biomed. Eng.* **2002**, *4*, 407−452.
(13) Nordhausen, C. T.; Maynard, E. M.; Normann, R. A. Single unit recording capabilities of a 100 microelectrode array. *Brain Res.* **1996**, *726* (1−2), 129−140.
(14) Eversmann, B.; Jenkner, M.; Hofmann, F.; Paulus, C.; Brederlow, R.; Holzapfl, B.; Fromherz, P.; Merz, M.; Brenner, M.; Schreiter, M.; Gabl, R.; Plehnert, K.; Steinhauser, M.; Eckstein, G.; Schmitt-Landsiedel, D.; Thewes, R. A 128x128 CMOS biosensor array for extracellular recording of neural activity. *IEEE J. Solid-State Circuits* **2003**, *38* (12), 2306−2317.
(15) Navarro, X.; Krueger, T. B.; Lago, N.; Micera, S.; Stieglitz, T.; Dario, P. A critical review of interfaces with the peripheral nervous system for the control of neuroprostheses and hybrid bionic systems. *J. Peripher. Nerv. Syst.* **2005**, *10* (3), 229−258.
(16) Xu, C. Y.; Lemon, W.; Liu, C. Design and fabrication of a high-density metal microelectrode array for neural recording. *Sens. Actuators, A: Physical* **2002**, *96* (1), 78−85.
(17) Bhat, S. V. *Biomaterials*, 1st ed.; Narosa Publishing House: New Delhi, India, 2002.
(18) Chawla, A. S. Evaluation of Plasma Polymerized Hexamethylcyclotrisiloxane Biomaterials Towards Adhesion of Canine Platelets and Leukocytes. *Biomaterials* **1981**, *2* (2), 83−88.
(19) Lewis, H. G. P.; Edell, D. J.; Gleason, K. K. Pulsed-PECVD films from hexamethylcyclotrisiloxane for use as insulating biomaterials. *Chem. Mater* **2000**, *12* (11), 3488−3494.
(20) Lewis, H. G. P.; Casserly, T. B.; Gleason, K. K. Hot-filament chemical vapor deposition of organosilicon thin films from hexamethylcyclotrisiloxane and octamethylcyclotetrasiloxane. *J. Electrochem. Soc.* **2001**, *148* (12), F212−F220.
(21) Chu, P. K.; Chen, J. Y.; Wang, L. P.; Huang, N. Plasma-surface modification of biomaterials. *Mater. Sci. Eng., R: Rep.* **2002**, *36* (5−6), 143−206.
(22) Favia, P.; d'Agostino, R. Plasma treatments and plasma deposition of polymers for biomedical applications. *Surf. Coat. Technol.* **1998**, *98* (1−3), 1102−1106.
(23) Lahann, J. Vapor-based polymer coatings for potential biomedical applications. *Polym. Int.* **2006**, *55* (12), 1361−1370.
(24) Yoshida, M.; Langer, R.; Lendlein, A.; Lahann, J. From advanced biomedical coatings to multi-functionalized biomaterials. *Polym. Rev.* **2006**, *46* (4), 347−375.
(25) Yasuda, H. *Plasma Polymerization*; Academic Press: 1985.
(26) Limb, S. J.; Gleason, K. K.; Edell, D. J.; Gleason, E. F. Flexible fluorocarbon wire coatings by pulsed plasma enhanced chemical vapor deposition. *J. Vac. Sci. Technol., A: Vac. Surf. Films* **1997**, *15* (4), 1814−1818.
(27) Pierson, H. O. *Handbook of Chemical Vapor Deposition*, 2nd ed.; William Andrew Publishing: Norwich, NY, 1999.
(28) Lau, K. K. S.; Gleason, K. K. Particle surface design using an all-dry encapsulation method. *Adv. Mater.* **2006**, *18* (15), 1972+.
(29) Chan, K.; Gleason, K. K. Initiated CVD of poly(methyl methacrylate) thin films. *Chem. Vap. Deposition* **2005**, *11* (10), 437−443.
(30) Mao, Y.; Gleason, K. K. Hot filament chemical vapor deposition of poly(glycidyl methacrylate) thin films using tert-butyl peroxide as an initiator. *Langmuir* **2004**, *20* (6), 2484−2488.
(31) Chan, K.; Gleason, K. K. Initiated chemical vapor deposition of linear and cross-linked poly(2-hydroxyethyl methacrylate) for use as thin-film hydrogels. *Langmuir* **2005**, *21* (19), 8930−8939.
(32) Lau, K. K. S.; Gleason, K. K. Initiated chemical vapor deposition (iCVD) of poly(alkyl acrylates): An experimental study. *Macromolecules* **2006**, *39* (10), 3688−3694.
(33) O'Shaughnessy, W. S.; Gao, M. L.; Gleason, K. K. Initiated chemical vapor deposition of trivinyltrimethylcyclotrisiloxane for biomaterial coatings. *Langmuir* **2006**, *22* (16), 7021−7026.
(34) Bradley, D. C.; Troyk, P. R.; Berg, J. A.; Bak, M.; Cogan, S.; Erickson, R.; Kufta, C.; Mascaro, M.; McCreery, D.; Schmidt, E. M.; Towle, V. L.; Xu, H. Visuotopic mapping through a multichannel stimulating implant in primate V1. *J. Neurophysiol.* **2005**, *93* (3), 1659−1670.
(35) Yamagishi, F. G. Investigation Of Plasma-Polymerized Films As Primers For Parylene-C Coatings On Neural Prosthesis Materials. *Thin Solid Films* **1991**, *202* (1), 39−50.
(36) Schmidt, E. M.; McIntosh, J. S.; Bak, M. J. Long-Term Implants Of Parylene-C Coated Microelectrodes. *Med. Biol. Eng. Comput.* **1988**, *26* (1), 96−101.

(37) Mark, J. E. *Polymer Data Handbook*; Oxford University Press: New York, 1999.
(38) Riande, E. *Electrical Properties of Polymers*; Marcel Dekker: New York, 2004.
(39) Troyk, P. R.; Watson, M. J.; Poyezdala, J. J. Humidity Testing Of Silicone Polymers For Corrosion Control Of Implanted Medical Electronic Prostheses. *ACS Symp. Ser.* **1986**, *322*, 299−313.
(40) Wang, D.; Ishida, H. Probing friction and adhesion properties of poly-(vinyl methylether) homopolymer and blend films under nano-confinement using atomic-force microscopy. *C. R. Chim.* **2006**, *9* (1), 90−98.
(41) Itagaki, H.; Nishimura, Y.; Sagisaka, E.; Grohens, Y. Entanglement of polymer chains in ultrathin films. *Langmuir* **2006**, *22* (2), 742−748.
(42) D. Lin-Vien, N. C.; W. Fately, J. Grasselli, *The Handbook of Infrared and Ramman Characteristic Frequencies of Organic Molecules*; Academic Press: San Diego, CA, 1991.
(43) Montgomery, D. C. *Design and Analysis of Experiments*; John C. Wiley & Sons: New York, 1997.
(44) Pollock, J. D.; Krempin, M.; Rudy, B. Differential-Effects Of Ngf, Fgf, Egf, Camp, And Dexamethasone On Neurite Outgrowth And Sodium-Channel Expression In Pc12 Cells. *J. Neurosci.* **1990**, *10* (8), 2626−2637.
(45) Murthy, S. K.; Olsen, B. D.; Gleason, K. K. Peptide attachment to vapor deposited polymeric thin films. *Langmuir* **2004**, *20* (11), 4774−4776.

BM070242S